Evaluation of Liquid-Solid Contacting in Trickle-Bed Reactors by Tracer Methods

The use of dynamic (tracer) methods for the evaluation of liquid-solid contacting and holdup in trickle-bed reactors is illustrated. It is shown that both the fraction of external catalyst area wetted and the fraction of total catalyst wetted by liquid can be obtained. External contacting efficiency and dynamic liquid saturation are correlated in terms of the appropriate dimensionless groups over the range of variables typical for trickle-flow operation. The relationship between catalyst contacting efficiency and catalyst utilization is outlined.

P. L MILLS

and

M. P. DUDUKOVIĆ

Chemical Reaction Engineering Laboratory
Department of Chemical Engineering
Washington University
St. Louis, MO 63130

SCOPE

Trickle-bed reactors are packed beds of catalyst with cocurrent flow of liquid and gas reactants and represent an important class of three phase reactors for gas-liquid contacting in the presence of a solid catalyst. Their use is widespread in the petroleum industry and potential applications in chemical processing, coal liquefaction, and waste water treatment are increasing. One of their advantages is an order-of-magnitude smaller power requirement in comparison to typical slurry reactors (Germain et al., 1978). Thus, it is not surprising that in the last five years several major review papers and monographs have addressed the various topics related to trickle-bed modeling and design (Satterfield, 1975; Goto et al., 1977; Hofmann, 1977, 1978; Gianetto et al., 1978; Shah, 1979). A consensus emerges that in order to predict trickle-bed performance and model its behavior, it is necessary to know what fraction of the catalyst is effectively wetted by the liquid phase (contacting efficiency) and the effectiveness factor of the resulting partly wetted catalyst. Unfortunately, catalyst contacting data taken on small porous particles typical of trickle-flow operation is very sparse (Satterfield, 1975; Schwartz et al., 1976; Colombo et al., 1976; Herskowitz et al., 1979). Furthermore, various measures of catalyst contacting and catalyst utilization have been defined and different methods have been proposed to evaluate them (Satterfield, 1975; Colombo et al., 1976; Schwartz et al., 1976).

Our objective is to develop efficient methods for determination of liquid-solid contacting. It is desired to evaluate the effect of liquid mass velocity on various measures of contacting efficiency and to determine whether contacting can be reliably determined from dynamic tracer tests. The effect of the catalyst packing activation state on the results obtained by dynamic testing is also sought. Evidence is presented, based on the work performed in this study, which show that dynamic tracer methods coupled with impulse or step response analysis can be used effectively to evaluate overall catalyst contacting by the flowing liquid. In addition, discrimination between reactor-scale and particle-scale incomplete contacting, external and internal contacting efficiency or partial pore fill-up can also be performed. Furthermore, the experimental data obtained in this study and that available in the literature is used to develop a correlation for external contacting and dynamic liquid holdup over the range of physical properties and flow rates typical for trickle-flow operation.

CONCLUSIONS AND SIGNIFICANCE

Proper interpretation of dynamic tests using nonvolatile liquid tracers provides information on both external and internal catalyst contacting in trickle-bed reactors. The fraction of internal catalyst area contacted by liquid can be obtained from the impulse response of an adsorbable tracer as proposed earlier by Schwartz et al. (1976). The variance of the impulse response for either a nonadsorbable or adsorbable tracer is related to the fraction of external catalyst area wetted in agreement with the method proposed by Colombo et al. (1976).

The fraction of internal catalyst area wetted (internal contacting efficiency) is unity over the whole range of liquid mass velocities studied (from 0.15 kg/m^{2}s to 3.5 kg/m^{2}s). The fraction of externally wetted area (external contacting efficiency) increases monotonically with liquid mass velocity and is unity only at highest velocities. An improved correlation for dynamic liquid holdup is presented in terms of appropriate dimensionless groups. A correlation for external contacting efficiency in terms of appropriate dimensionless groups has been developed based on the data of this study and that available in the literature.

The effect of the catalyst packing activation state on tracer adsorption is illustrated and the accuracy of the tracer method is demonstrated.

CONTACTING EFFICIENCY AND CATALYST UTILIZATION

Some ambiguity exists in the literature as to the definition of liquid-solid contacting efficiency (effectiveness) and catalyst utilization in trickle-bed reactors. The fraction of external catalyst area wetted by liquid η_{CE}, the fraction of total catalyst area (internal and external) wetted η_C, the fraction of internal catalyst area wetted η_i, and fractional pore fill-up F_i are each an estimate of contacting efficiency, yet at given conditions they all may have different values. Various experimental methods determine different measures of contacting and thus care should be taken to properly identify which measure of contacting is being evaluated.

Satterfield's (1975) method of taking the ratio of the apparent rate constants obtained in trickle-flow operation to the one determined using the same catalyst under conditions of complete external and internal wetting is also called contacting

P. L. Mills is with the General Electric Co., General Electric Research and Development Center, Schenectady, NY 12301

0001-1541-81-4910-0892-$2.00.

effectiveness but is really a measure of catalyst utilization. This measure represents the ratio of the effectiveness factors for the catalyst in both the trickle-bed and the liquid-full reactor. In the case of a large Thiele modulus (low effectiveness factor for completely wetted pellet), catalyst utilization is related to external contacting efficiency. Under certain circumstances, the catalyst utilization will be directly proportional to either the fraction of externally wetted area for nonvolatile liquid limiting reactants (Dudukovic, 1977; Mills and Dudukovic, 1980) or directly proportional to the fraction of externally dry area in the case of gas limiting or volatile liquid limiting reactants (Herskowitz et al., 1979; Mills and Dudukovic, 1980). When the Thiele modulus is small, catalyst effectiveness factors are almost unity for completely wetted catalysts so that catalyst utilization is proportional to internal contacting efficiency or internal pore fill-up (Dudukovic, 1977). When the apparent rate of reaction in trickle-flow is determined by a combination of gas-to-liquid, gas-to-solid, and liquid-to-solid external mass transfer resistances, then catalyst utilization is a function of external contacting efficiency. As a consequence, the measure of catalyst contacting which is representative of catalyst utilization depends on the kinetic regime and limiting reactant.

It has been assumed in the above discussion that only particle-scale incomplete contacting is present in the reactor. When only reactor scale incomplete contacting is present due to global maldistribution of liquid flow, some areas of the reactor may be completely dry while in other areas the catalyst particles are completely externally and internally wetted. All of the above defined measures of catalyst contacting yield now the same result. For the case of nonvolatile liquid limiting reactants catalyst utilization can properly be represented by the fraction of the reactor that is completely wetted. When both particle scale and reactor scale incomplete contacting occur it is difficult to determine various measures of contacting from the tracer or reaction tests alone. Comparison of tracer tests in liquid-full and trickle-flow reactor may yield this information as shown in this paper.

EVALUATION OF LIQUID-SOLID CONTACTING

Methods

Several methods have been proposed in the literature which allow experimental assessment of liquid-solid contacting. They may be basically divided into two categories: (i) destructive methods and (ii) nondestructive methods. Destructive methods either require a change in the nature of bed packing or special choice of the flowing phase, or require dismantling of the bed for the experiment to be performed. Examples include nonreactive synthetic packing dissolution methods (Shulman, 1955) for estimation of external contacting, direct measurement of contacted area by permanent dye adsorption (Onda, 1967; Krauze and Serwinski, 1971), and determination of externally contacted area by dissolution of synthetic packing with a reacting buffer solution (Specchia et al., 1978). Nondestructive techniques rely on dynamic tracer tracing. These include determination of liquid holdup and fractional pore fill-up (Lapidus, 1957; Schiesser and Lapidus, 1961), evaluation of total catalyst area contacted by comparison of dynamic impulse responses for nonadsorbing and adsorbing tracers (Schwartz, et al., 1976), and determination of liquid-solid external contacting efficiency by comparison of dynamic responses in two-phase flow to liquid-full operation (Colombo et al., 1976). As discussed earlier, Satterfield's (1975) ratio of rate constants k_{app}/k_v based on reaction data in both a two-phase flow and liquid-full reactor, as used by Koros (1976) and Herskowitz et al. (1979), is a direct measure of external contacting efficiency only in case of very low catalyst effectiveness factors.

The destructive methods described above have had success in producing useful correlations for absorption columns packed with large nonporous packing ($d_p > 1.27$ cm or ½ in.). There is no correlation for external contacting which is based on data for small porous catalyst particles [0.079 cm (1/32 in.) $\leq d_p \leq$ 0.159 cm (1/16 in.)] obtained for flow regimes and physical properties typical for trickle-flow operation. The state of the art in predicting external contacting is given by the summary of empirical processing data on k_{app}/k_v in Figure 4 of Satterfield's paper (1975) which has been reproduced by most review papers that followed.

The tracer techniques mentioned above seem to be more promising in rapidly producing contacting information which is more representative of commercial processes than the destructive methods. Among the tracer methods, those of Colombo et al. (1976) and Schwartz et al. (1976) are the most current. Colombo et al. (1976) express liquid-solid contacting efficiency by the ratio of the apparent diffusivity $(D_{eo})_{app}$ of the tracer in a porous particle in a trickle-bed reactor to the diffusivity $(D_{eo})_{LF}$ obtained in a liquid-full reactor. Diffusivities are obtained from the first moment of a step response, or equivalently, from the variance of the impulse response. The interpretation of results relies on the assumption that catalyst particles are internally completely wetted and it is argued, based on reduced external area for transport and increased diffusion path length (but not proven) that $(D_{eo})_{app}/(D_{eo})_{LF} = \eta_{CE}$. Schwartz et al. (1976) use the ratio of the apparent equilibrium constant $(K_A)_{app}$ of a linearly adsorbing tracer as determined in a trickle-bed reactor to the adsorption equilibrium constant $(K_A)_{LF}$ obtained from totally wetted pellets. The method uses the first moment of the impulse response curves for both adsorbing and nonadsorbing tracers and claims to determine the fraction of total catalyst area contacted. Both approaches are used and compared in the present study.

Interpretation of Tracer Data

Responses to impulse injections of both nonvolatile adsorbing and nonadsorbing tracers in the liquid are used in this study to obtain information on liquid holdup, fraction of internal catalyst area contacted, and external contacting efficiency. If a particular model for the reactor is assumed, direct time-domain parameter estimation is possible (Mills, 1980) and will be subject of a future publication. Here, the objective is to illustrate and compare the methods of Schwartz et al. (1976) and Colombo et al. (1976) using the method of moments to determine the above parameters. The axial dispersion model is assumed for the transport of tracer in the reactor coupled with external mass transfer and diffusion with/without fast adsorption in each catalyst particle. The pertinent equations and the algebra involved in finding the moments are well known (Schneider and Smith, 1968; Suzuki and Smith, 1971; Colombo et al., 1976; Mills, 1980) and only the final results for the first moment and variance of a normalized impulse response for a nonvolatile tracer are presented below.

The expression for the first moment presented below is derived based on the assumption that solid catalyst is incompletely wetted:

$$\mu_1 = \frac{V_R}{Q_L}\left[H_L + F_i(1-\epsilon_B)\epsilon_P\left(1+\frac{K_A\rho_P}{\epsilon_P}\right)\right] = \frac{V_R H_T}{Q_L} + \frac{V_R(1-\epsilon_B)(K_A)_{app}\rho_P}{Q_L} \quad (1)$$

Due to assumptions used in deriving this expression, the fractional pore fill up F_i, and internal catalyst contacting efficiency η_i may be used interchangeably. Furthermore, in the case of typical porous catalysts, the internal surface area which is available for tracer adsorption dominates over the external area of the particles (e.g., 232 m²/g vs. 0.003 m²/g for the 20-28 mesh Alcoa F-1 alumina used in this study). This suggests that the ratio of the apparent adsorption equilibrium constant observed in two-phase flow $(K_A)_{app}$ to the adsorption equilibrium constant determined for completely wetted particles (such as in a batch experiment or in a liquid filled column) K_A, is a measure of

internal catalyst contacting efficiency, n_i. This is due to the dominance of internal surface area over the external surface area so that the internal contacting efficiency n_i is indistinguishable from total catalyst contacting efficiency n_C.

In order to apply the method of Schwartz et al. (1976) it is necessary to perform experiments with nonadsorbing tracers ($K_A = 0$) to determine total liquid holdup H_T. This is followed by experiments with adsorbing tracers in order to find $(K_A)_{app}$ from which contacting efficiency is determined. For liquid-full reactors, Eq. 1 is still valid when bed porosity ϵ_B replaces external liquid holdup H_L, total porosity $\epsilon_B + (1 - \epsilon_B)\,\epsilon_P$ replaces total liquid holdup H_T, true adsorption equilibrium constant $(K_A)_{LF}$ replaces $(K_A)_{app}$, and F_i equals one. Internal contacting efficiency is then obtained by comparing the difference in first moments for adsorbing and nonadsorbing tracers in two phase flow to their difference in liquid filled operation:

$$\eta_i = \frac{(\mu_{1,ad})_{TP} - (\mu_{1,n.ad})_{TP}}{(\mu_{1,ad})_{LF} - (\mu_{1,n.ad})_{LF}} = \frac{(K_A)_{app}}{(K_A)_{LF}} \tag{2}$$

Two adsorbing tracers with a sufficient difference in adsorption constants can be used alone.

The method of Colombo et al. (1976) relies on the use of the variance of the impulse response (the first moment of a step response was used in the original paper which is equivalent to the approach presented here) and is based on the assumption that internal wetting is complete and thus $K_A = (K_A)_{app}$. Under these conditions, and assuming negligible adsorption resistance, the expression for the variance of the impulse response obtained in two-phase flow operation can be written as:

$$\frac{\sigma^2}{2\mu_1^2} = \frac{Q_L}{V_R H_L}\,\frac{\delta_1}{(1+\delta_0)^2} + \frac{1}{Pe_L} \tag{3}$$

where:

$$\delta_1 = \delta_i + \delta_e \tag{4}$$

$$\delta_i = \frac{(1-\epsilon_B)\epsilon_P}{H_L}\left[1 + \frac{K_A\rho_P}{\epsilon_P}\right]^2 \frac{R^2\epsilon_P}{15}\,\frac{1}{(D_{eo})_{app}} \tag{5}$$

$$\delta_e = \frac{(1-\epsilon_B)\epsilon_P}{H_L}\left[1 + \frac{K_A\rho_P}{\epsilon_P}\right]^2 \frac{R^2\epsilon_P}{15}\,\frac{5}{k_{LS}R} \tag{6}$$

$$\delta_0 = \frac{(1-\epsilon_B)\epsilon_P}{H_L}\left[1 + \frac{K_A\rho_P}{\epsilon_P}\right] \tag{7}$$

In the case of liquid-full operation, bed porosity ϵ_B replaces external liquid holdup H_L, and the effective diffusivity for a liquid-full reactor $(D_{eo})_{LF}$ replaces the apparent diffusivity $(D_{eo})_{app}$ observed in two-phase flow. The original paper by Colombo et al. (1976) asserts that the ratio $(D_{eo})_{app}/(D_{eo})_{LF}$ is equal to external contacting efficiency. This heuristic argument at first seems acceptable since in the derivation of the above equations the effective diffusivity is based on total catalyst area, and, thus, for two-phase flow, contains in itself a correction factor proportional to the fraction of external area wetted. Later, Baldi (1980) modified the above statement. By equating the Thiele modulus for a partly wetted catalyst pellet, based on the measured $(D_{eo})_{app}$ and on actual geometric volume and external surface of the pellet, to the modulus for partly wetted pellets as defined by Duduković (1977), under the assumption of complete pore fill-up, $\eta_i = 1$, Baldi (1980) arrives to the conclusion that the *square root* of the ratio $(D_{eo})_{app}/(D_{eo})_{LF}$ equals external contacting efficiency. It should be pointed out, however, that a complete rigorous solution to the transient diffusion problem in a spherical particle that is incompletely wetted on the external surface has not been presented to date. For that reason, the rigorous proof of the relationship between $(D_{eo})_{app}/(D_{eo})_{LF}$ and external contacting efficiency is still lacking.

In order to interpret tracer response data for Colombo's model (1976) by the method of moments, one must evaluate effective diffusivities in liquid-full and two-phase flow operation and in the process estimate Peclet numbers and liquid-solid mass transfer coefficients. For liquid-full operation, Peclet numbers are obtained in this study from the Chung and Wen (1968) correlation and mass transfer coefficients are estimated from the correlation of Dwivedi and Upadhyay (1977). Upon substituting these correlations into Eq. 3, the following form is obtained:

$$\frac{\sigma^2}{2\mu_1^2} = \left(\frac{\delta_0}{1+\delta_0}\right)^2 \frac{\epsilon_B}{\epsilon_P(1-\epsilon_B)}\,\frac{R^2\epsilon_P}{15}\left[\frac{Q_L}{V_R\epsilon_B D_{eo}} + \frac{5}{1.1068}\,\frac{A_R Sc_L^{2/3}}{V_R R}\left(\frac{Q_L d_P \rho_L}{A_R \mu_L}\right)^{0.72}\right] + C_1\,\frac{d_P A_R}{V_R \epsilon_B} \tag{8}$$

The last term in Eq. 8 demonstrates that only the constant term of the Chung and Wen (1968) Peclet number correlation is found to be significant at conditions of this study ($Re_L < 10$). The correlation suggests $C_1 = 5$, but since the nature of packed beds vary this constant is left as an undetermined parameter. It can be determined by simultaneous nonlinear regression of the volumetric flow rate and dimensionless variance data pairs.

For two-phase flow, Peclet numbers can be estimated from the correlation of Hochman and Effron (1969) or Buffham and Rathor (1978) while mass transfer coefficients can be obtained from the correlation of Specchia et al. (1978) or Goto and Smith (1975).

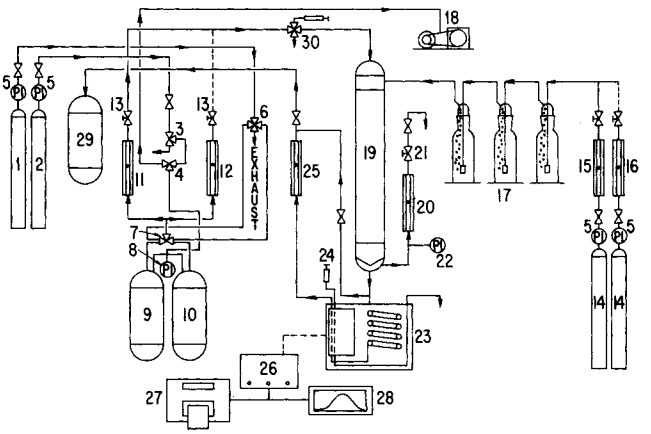

Figure 1. Experimental equipment for tracer studies.

TABLE 1. LIST OF KEY EQUIPMENT ITEMS

No.	Item	No.	Item
1	Step Valve Supply Pressure Cylinder	15	Low Range Gas Flowmeter
2	Feed Tank Supply Pressure Cylinder	16	High Range Gas Flowmeter
3	3-Way Ball Valve (Pressure/Bleed)	17	Inlet Gas Bubblers
4	3-Way Ball Valve (Pressure/Vacuum)	18	Vacuum Pump
5	Cylinder Pressure Indicator and Regulator	19	Trickle-Bed Column
6	4-Way Ball Valve	20	Outlet Gas Flowmeter
7	3-Way Pneumatic Switching Ball Valve	21	Outlet Gas Metering Valve
8	Feed Tank Pressure/ Vacuum Gauge	22	Column Pressure Indicating Gauge
9	Solvent Supply Tank	23	Refractometer Water Bath
10	Solvent/Tracer Supply Tank	24	Refractometer Reference Side Liquid
11	Low Range Liquid Flowmeter	25	Refractometer Outlet Liquid Flowmeter
12	High Range Liquid Flowmeter	26	Control Module
13	Liquid Inlet Metering Valve	27	Voltmeter/Printer/ Microprocessor
14	Inlet Gas Supply Cylinders	28	Recorder
		29	Waste Tank
		30	Tracer Injection Valve

Experimental Apparatus and Procedure

The experimental apparatus used in this study is represented schematically in Figure 1 and described in Table 1. Both impulse injections (30) (sample loop volume = 0.606 cm^3) and step changes activated by a three-way pneumatic switching ball valve (7) are possible. For two-phase operation, carrier gas (helium) is saturated with carrier liquid (hexane) in a set of bubblers (17) while the carrier liquid (hexane) is kept under carrier gas (helium) pressure in a tank (9). This eliminates gas-liquid exchange in the column. All flow rates are carefully controlled and monitored by rotameters. The exit liquid stream is passed through the optical block of the Waters R-403 differential refractometer immersed in a highly accurate Tronac CTB-405 temperature bath. The major modifications of the refractometer included installation of a coil for temperature equilibration of the liquid stream prior to entry in the optical block. The resulting superior performance of the instrument in terms of high baseline stability and fine resolution are described in a previous publication (Mills and Duduković, 1979).

The output signal from the control module of the refractometer consists of a continuous 100 mV analog source. The tracer response curves are always displayed on a ten-inch Beckman strip-chart recorder for visual assessment of the particular experiment as it progresses from start to finish. A quartz crystal-controlled clock is tuned to the AC voltage line source frequency and an Analog Devices STX 2603 microprocessor has been used to convert the BCD signal from the digital meter to asynchronous ASC11 format to drive an ASR 33 EIA teletype. The output signal from the control module of the refractometer is then punched by the teletype onto paper tape at selected discrete time intervals as the experiment proceeds. The teletype is then rolled to one of the available ports of the Engineering School DEC-20 computer and read directly into a data file with special computer software for direct signal processing. As many as twenty data sets each containing a minimum of 500 points could be recorded and stored in a single day as a result of this procedure which represented a dramatic improvement over the previous procedure of manually keypunching the data. Further details are provided by Mills (1980).

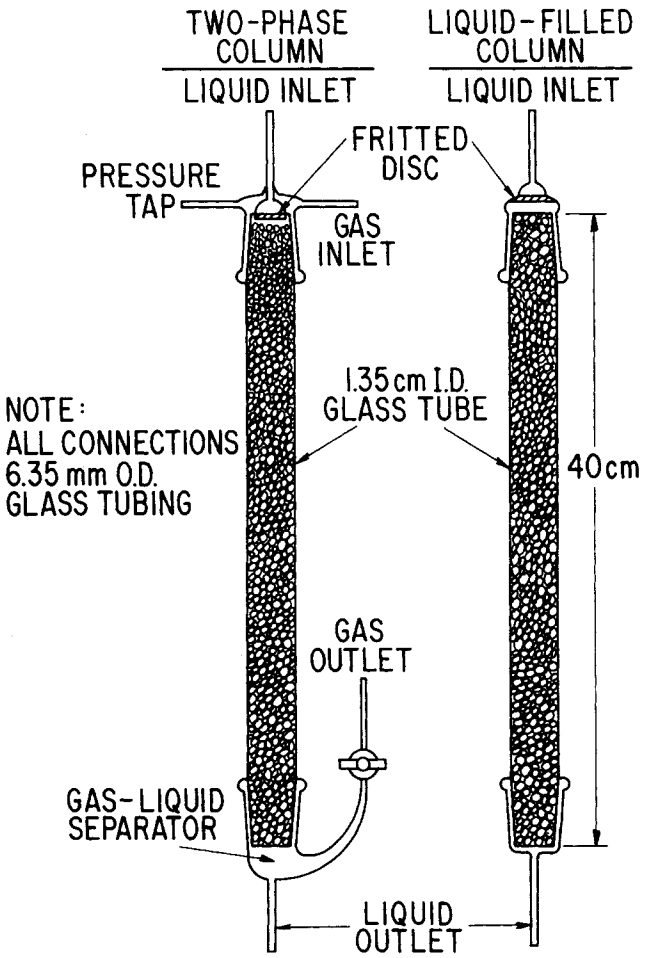

Figure 2. Experimental trickle-bed reactor.

The teletype and paper tape can be readily bypassed if the signal could be introduced directly to the DEC-20 provided that additional hardware were available. Alternately, the data could be stored directly on magnetic tape. However, a magnetic tape drive is often too costly due to budgetary limitations and additional ports for direct computer linkage are either not available or are also prohibitively costly. In such a case, the above solution was found to be extremely cost effective and satisfactory.

The same packed bed is used in all liquid-full and two-phase flow experiments (Figure 2). In this study, the results obtained on 20-28 mesh Alcoa F-1 alumina are presented. Bed porosity was determined to be $\epsilon_B = 0.374$ while pellet porosity $\epsilon_P = 0.495$ with an average pore radius of 27 Å. Average particle size is 0.0718 cm. Complete physical properties of all the packings used are reported by Mills (1980).

Three types of packing activation were used: i) non-activated packing; (ii) packing exposed to flowing dry helium; and (iii) packing activated in situ by exposure to flowing dry helium and maintained at temperatures of up to 250°C. All experiments are performed with preflooded beds. Hexane is used as a carrier fluid (Fisher Scientific Company ACS reagent grade) but has been purified in our laboratory by passing over activated carbon and activated alumina. Pentane, heptane, cyclohexane, cyclohexene, para-xylene, tetrahydronaphthalene, and other similar organic compounds are used as tracers. The range of operating variables covered is $0.33 < Re_L < 7.91$; $0.146\ (kg/m^2s) < L_m < 3.48\ (kg/m^2s)$ and $1.19 \times 10^{-3}\ (kg/m^2s) < G_m < 1.98\ (kg/m^2s)$.

Multiple experiments are performed at each of the several selected liquid flow rates for both liquid-filled column and two-phase flow operation. Repeated experiments are performed at the same flow rate with the packed bed removed and the inlet and outlet column heads (Figure 2) connected together in order to determine the response of all the lines between the tracer injection point and optical block of the refractometer. The subtraction of the corresponding moments for these injection-sampling system experiments from the ones obtained with liquid-full or two-phase columns in place allows the moments for the packed bed to be determined. Further details concerning the purification of chemicals and experimental procedure are given by Mills (1980).

Data Analysis

Various computer software was developed for tracer data processing specifically for: (i) transformation of output voltages from the analytical equipment to a computer compatible form; (ii) storage of raw experimental data for future signal processing; (iii) evaluation of the stored experimental data by the method of moments; and (iv) evaluation of the stored experimental data by time-domain analysis.

The theoretical expressions for the moments in terms of unknown parameters $(K_A)_{LF}$ or $(K_A)_{app}$ and $(D_{eo})_{LF}$ or $(D_{eo})_{app}$ are given by Eqs. 1 and 3. The moments of the experimental curve are defined by:

$$\mu_n = \frac{\int_o^\infty t^n C_L dt}{\int_o^\infty C_L dt} \tag{9}$$

and

$$\sigma^2 = \mu_2 - \mu_1^2 \tag{10}$$

Since the first moment and the variance are additive for linear systems, the moments corresponding to the response of the packed bed (subscript C) are obtained by the following subtraction:

$$(\mu_1)_C = (\mu_1)_D - (\mu_1)_{D.V.} \tag{11}$$

$$(\sigma^2)_C = (\sigma^2)_D - (\sigma^2)_{D.V.} \tag{12}$$

The subscript D indicates the moments obtained from a response with the packed bed in place, and subscript $D.V.$ refers to the moments of the injection-sampling system response. Since the relationship between tracer concentration and output voltage is linear, the moments given by Eq. 9 can be obtained by direct numerical integration of the stored output voltage data for a particular experimental run. A data reduction program called TBR (Mills, 1980) was developed for this purpose. Program TBR is a complete program for the analysis of tracer responses. It includes data input and editing, numerical inte-

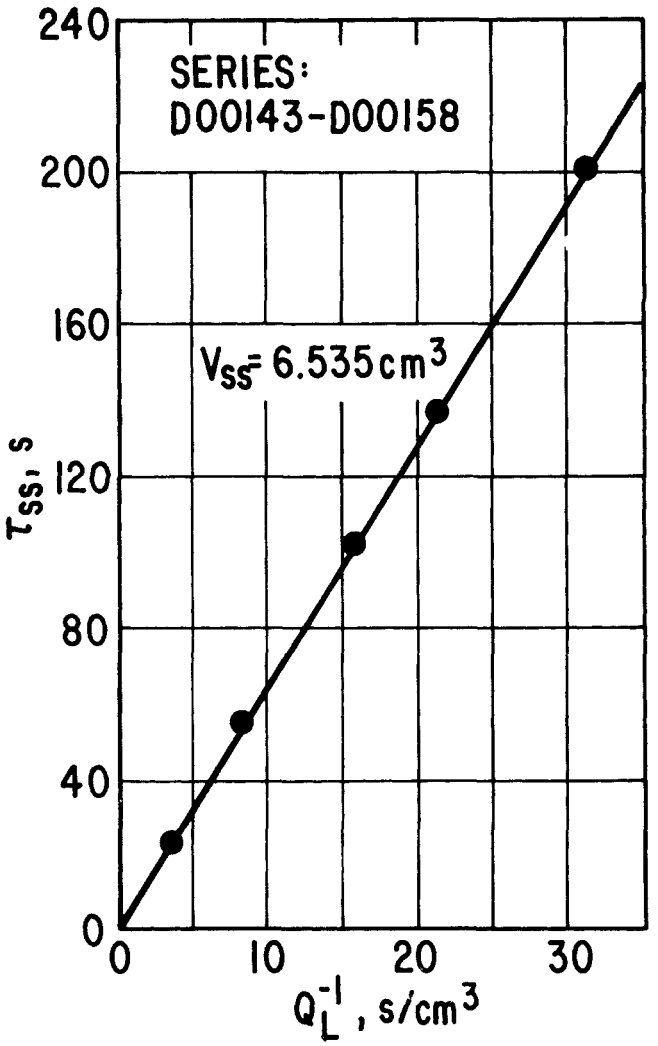

Figure 3. Mean residence time of the combined injection-sampling system for two-phase operation as a function of flow rate.

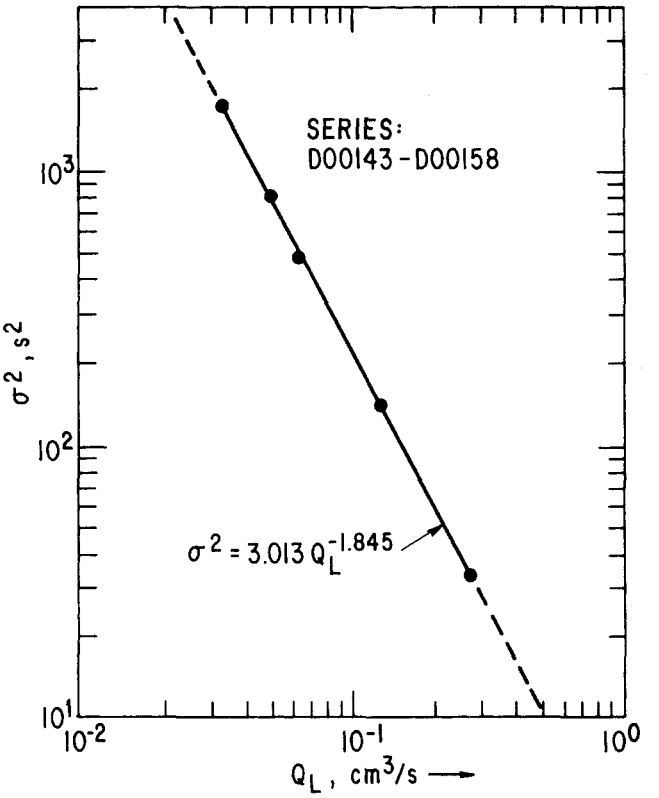

Figure 4. Variance of the combined injection-sampling system for two-phase operation as a function of flow rate.

gration of the time-voltage curve including computer graphics display for ease in exponential decay tail extrapolation, calculation of unknown parameters, and output of data and parameters in tabular form. It may be used to evaluate the moments for either pulse, step-up or step-down response data. It also includes options for: (i) smoothing of noisy data by cubic-spline analysis; (ii) correction of the baseline for long term drift; (iii) calculation of the age density functions; and (iv) storage of results for subsequent processing if needed. Complete documentation is presented by Mills (1980).

RESULTS AND DISCUSSION

Injection Sampling System Response

The most demanding test of the tracer method is when the volume of the system to be tested is small. For this reason, impulse tracer experiments were first performed using the combined injection valve, valve-to-column inlet tubing, capillary coil in the temperature bath, and associated fittings as the system. The volume of the system was accurately determined by filling and draining with liquid to be 3.84 cm^3. Tracer tests were performed at a number of flow rates and the first moment was plotted against reciprocal flow rate. A straight line was obtained whose slope gave a value of 3.935 ± 0.225 cm^3 for the system volume. This was within 2.5% of the measured volume. The same type of tracer experiments were performed for the whole injection-sampling system including specially fabricated heads which simulate the available liquid head space in two-phase flow. The results for the first moment (τ_{ss}) and variance (σ^2) are given in Figures 3 and 4. Similar results were obtained using the heads for liquid-full operation (which contains a somewhat larger liquid space). For liquid-full operation, the external volume with respect to the packed bed was V_{ss} = 6.535 cm^3 and the empirical equation for the variance was $\sigma^2 = 3.013\, Q_L^{-1.845}$.

It should be pointed out that in Figures 3 and 4 and all subsequent Figures every data point represents a mean value of several repeated experiments with the error bars, i.e., variation of values on which the mean is based. These are well within the symbol for the data point unless otherwise indicated.

Liquid-Full Experiments

The objective of the liquid-full tests was to: (i) establish that tracer based values of the bed active volume were reliable, and examine the effect of water adsorption on these values; (ii) determine the adsorption equilibrium constant $(K_A)_{LF}$ for totally wetted pellets using a suitable tracer and examine the effect of the packing's state-of-activation on this value; and (iii) determine the effective diffusivities $(D_{eo})_{LF}$ for both an adsorbing and nonadsorbing tracer.

A series of tracer tests was first performed in a liquid-filled column using F-1 alumina to determine the role of water and the packing activation state on tracer accessible volume. Heptane was selected as a suitable nonadsorbing tracer. The bed was packed with 55.2604 grams of alumina which had been exposed to humid laboratory air. The packing was neither heated nor exposed to dry helium. The bed was flooded for 24 hours and tracer tests performed. From the results presented in Figure 5, a tracer accessible liquid volume of 38.034 ± 0.286 cm^3 was determined. When the volume of sampling system was subtracted, a hexane fractional pore fill-up of 0.716, i.e., 71.6% was obtained. The bed was then drained and dry helium was passed through the bed for 24 hours at room temperature followed by another prewetting procedure. The repeated tracer runs yielded a value of 42.473 ± 0.664 cm^3 as a tracer accessible volume for a fractional pore fill-up of 0.993 or 99.3%.

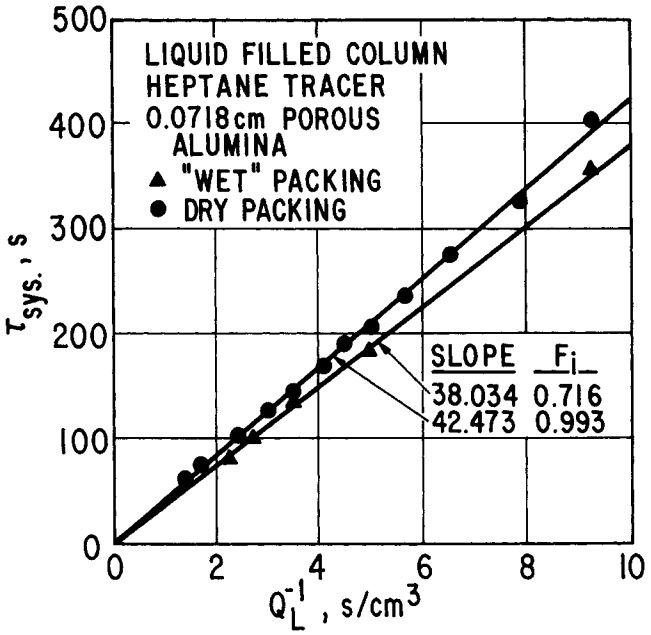

Figure 5. Comparison of mean residence times for heptane tracer using wet and dry porous F-1 alumina.

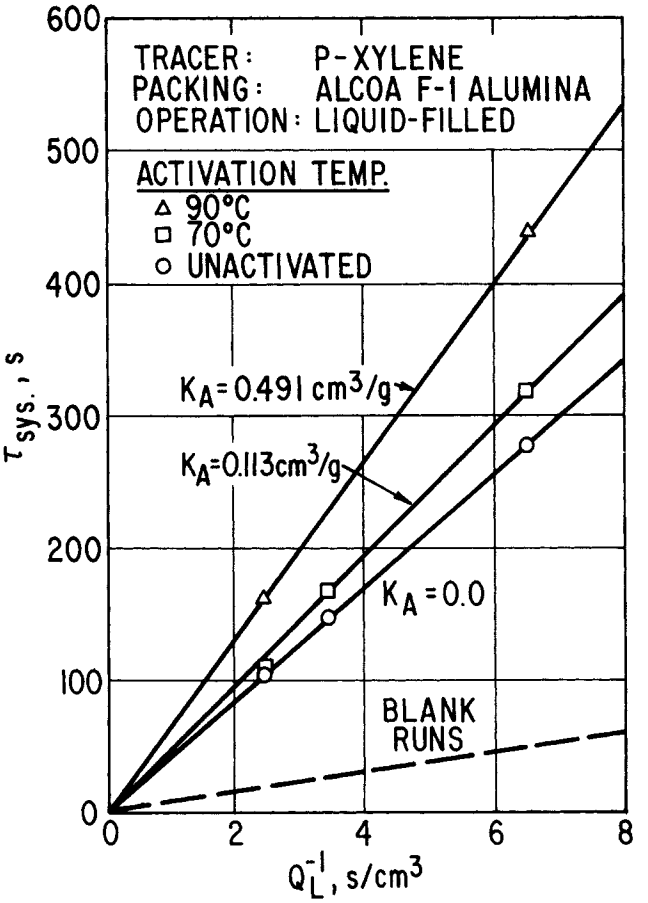

Figure 6. Effect of packing activation temperature on adsorption equilibrium constants for para-xylene tracer.

The bed was drained, dried at room temperature in presence of helium, and weighed to give 50.9585 grams of packing. The amount of water of 4.3019 grams driven off by helium occupies 26.9% of the pore volume leaving 73.1% available to hexane which is in excellent agreement with the tracer determined value of 71.6% for the original bed.

Another set of runs was performed using para-xylene as a tracer while the same packed bed was used in three different states of activation. These included: (i) an unactivated state in which the bed was only exposed to dry helium for 24 hours at room temperature; (ii) an activated state in which the packing was exposed (in situ) to dry helium at 70°C; and (iii) an activated state in which the bed was treated with helium at 90°C. The results for the first moment are presented in Figure 6 where the "blank runs" indicate the first moment for the injection-sampling system. The slope of the lower line (K_A = 0.0) is 42.177 cm^3 which is within 0.7% of the liquid volume determined by heptane tracer (Figure 5). This confirms that the results are tracer independent. Activating the packing at 70°C (K_A = 0.113 cm^3/g) resulted in a slight adsorption of tracer while heating at 90°C increased K_A four-fold (K_A = 0.491 cm^3/g). Heating the packing further to 250°C resulted in irreversible adsorption of para-xylene, i.e., no tracer was detected in the outflow upon repeated impulse injections into the system.

Additional liquid-full runs were performed over a wider range of liquid flow rates and are summarized in Table 2 and in Figure 7. The tracer based volumes (using nonadsorbing tracers) yield results which are within the accuracy with which the bed porosity ϵ_B, pellet porosity ϵ_P, reactor volume V_R, and injection-sampling system V_{ss} are determined. Similar results (not shown here) for the available liquid volume were obtained for a column packed with glass beads. As expected, n-heptane and n-pentane yield identical results (Figure 7) but somewhat surprisingly even they are weakly adsorbed (K_A = 0.125) on fully activated F-1 alumina. Pentane or heptane on nonactivated helium dried alumina and cyclohexene on fully activated alumina are therefore possible choices for nonadsorbing and adsorbing tracers, respectively.

Effective diffusivities of pentane and cyclohexene corresponding to cases 2 and 4 in Table 2 were evaluated from the expression for the variance given by Eq. 8. The remaining unknowns $(D_{e0})_{LF}$ and C_1, i.e., Pe_L, were calculated by nonlinear regression. The results are shown in Figure 8 where the dimensionless variance $\sigma_\theta^2 = \sigma^2/\mu_1^2$ is plotted as a function of liquid volumetric flow rate Q_L. The full curves represent the values calculated based on the estimated parameters. The average error between the fitted line and experimental values of the

TABLE 2. SYSTEMS STUDIED IN LIQUID FULL TESTS

Case	Packing	Bed Porosity ϵ_B	Particle Porosity ϵ_P	Tracer	Activation State	Volume (cm^3) Tracer	Volume (cm^3) Calculated	% Error	K_A (cm^3/g)
1	T-61/F-1 alumina	0.425	0.08	n-heptane	activated	31.6 ± 0.4	31.6 ± 0.4	−1.6	0
2	F-1 alumina	0.374	0.495	n-pentane	helium dried	43.4 ± 0.7	42.6 ± 0.6	+1.9	0
3	F-1 alumina	0.374	0.495	n-pentane	activated	49.0 ± 1.6	—	—	0.125
4	F-1 alumina	0.374	0.495	n-heptane cyclohexene	activated	64.3 ± 1.6	—	—	0.427

In all cases the volume of the reactor is 51.6 cm^3

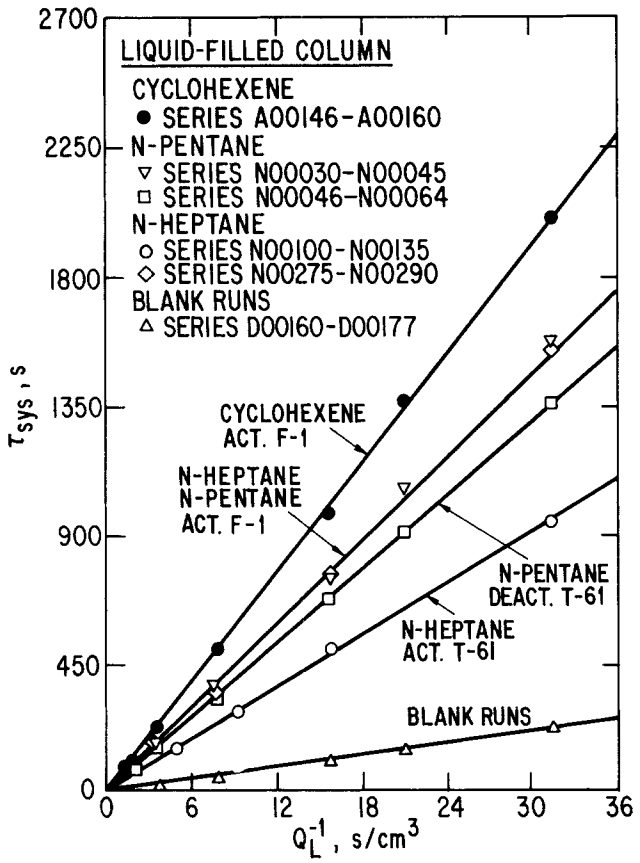

Figure 7. First absolute moments for various tracers in a liquid-filled column for various alumina packings.

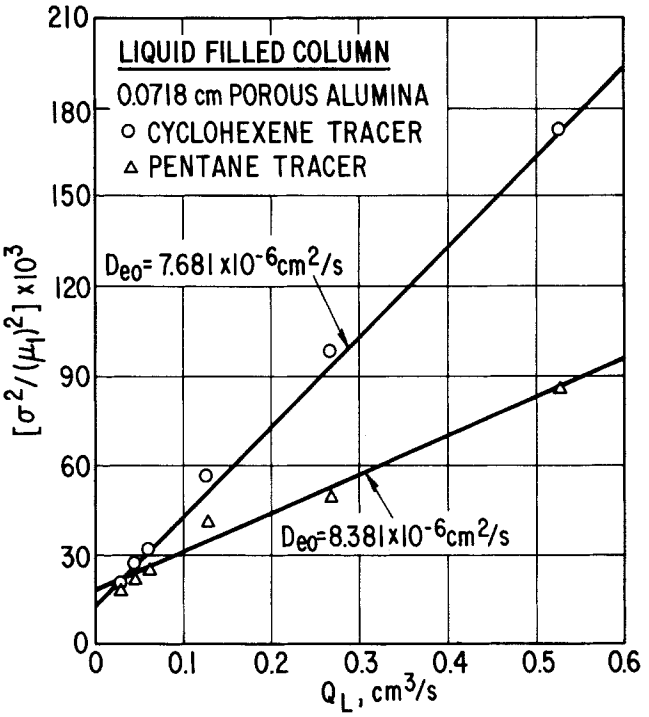

Figure 8. Effective diffusivities for cyclohexene and n-pentane tracers in porous F-1 alumina.

dimensionless variance is 2.6% for pentane and 1.5% for cyclohexene. The effective diffusivity for pentane was found to be 8.381×10^{-6} cm^2/s and 7.681×10^{-6} cm^2/s for cyclohexene. The molecular diffusivities when estimated from Wilke-Chang correlation as reported by Reid et al. (1977) for pentane in hexane and cyclohexene in hexane are 3.66×10^{-5} cm^2/s and 3.84×10^{-5} cm^2/s, respectively. The tortuosity factor based on pentane data (nonadsorbing tracer) is 2.2, while a value of 2.5 is obtained from cyclohexene data (adsorbing tracer). Since the two are within experimental error, it is not possible to tell whether pore diffusion of the adsorbing tracer is somewhat more hindered. The relative importance of liquid-to-solid mass transfer resistance to the combined liquid-to-solid plus internal diffusion resistance ($\delta_e/(\delta_e + \delta_i)$) is about 23% at the lowest flow rate (Q_L = 0.032 cm^3/s) and about 11% at the highest flow rate (Q_L = 0.527 cm^3/s). The reproducibility of the variance, from which effective diffusivity is calculated, is excellent. The largest variations are encountered at the lowest liquid flow rate (Q_L = 0.032 cm^3/s) where three repeat injections with cyclohexene produced values of 0.0207, 0.0197 and 0.0197 for the dimensionless variance.

Two-Phase Flow Experiments

The objective of the two-phase flow experiments was to: (i) obtain total external and dynamic liquid holdup for comparison to the data and correlations available in the literature; (ii) determine the effect of liquid flow rate, if any, on catalyst contacting as obtained by the method of Schwartz et al. (1976); and (iii) establish the effect of liquid flow rate on catalyst contacting as obtained by the method of Colombo et al. (1976). The most recent investigations for liquid holdup and liquid-solid contacting in trickle-flow over beds of small porous particles are summarized in Table 3. The range of operating variables over which these investigations were performed are shown on the flow map of Charpentier and co-workers (1976) in Figure 9. All of the studies according to this flow map were performed in the trickle flow regime. The transition to pulsing flow was visually observed in this work at the highest liquid velocities but is not so indicated by examination of this figure.

a. Liquid Holdup. Total liquid holdup was obtained from Eq. 1 using nonadsorbing tracers such as pentane and heptane on unactivated, helium dried F-1 alumina or cyclohexane on relatively non-porous T-61 alumina (ϵ_P = 0.026, ϵ_B = 0.466). The holdup results are plotted as function of liquid flow rate in Figure 10. The solid lines were determined by fitting the data to the relationship given below which was proposed by Satterfield and Way (1972):

Table 3. Summary of Recent Liquid Holdup and Solid-Liquid Contacting Investigations for Small Porous Packings

Investigation	Packing	Item(s)	Re_L	$Fr_L \times 10^4$	$We_L \times 10^7$
Goto and Smith (1975)	0.0541 cm CuO · ZnO	H_D	0.29 – 3.0	1.4 – 153	5.1 – 556
	0.291 cm CuO · ZnO		1.55 – 16.1	0.3 – 29	27 – 2927
Colombo et al. (1976)	0.1 cm act. carbon	H_D,?η_{CE}	0.57 – 7.8	1.2 – 220	10.9 – 2021
	0.38 cm × 0.48 cm carbon cylinders		2.3 – 31.9	0.3 – 49.0	49 – 9073
This work	0.0718 cm Al_2O_3	H_D,?η_{CE}, η_i	0.33 – 7.5	0.3 – 133	3.4 – 1722
Herskowitz et al. (1979)	0.162 cm Pd on Al_2O_3	η_{CE}	1.07 – 42.9	0.48 – 765	38.8 – 61980

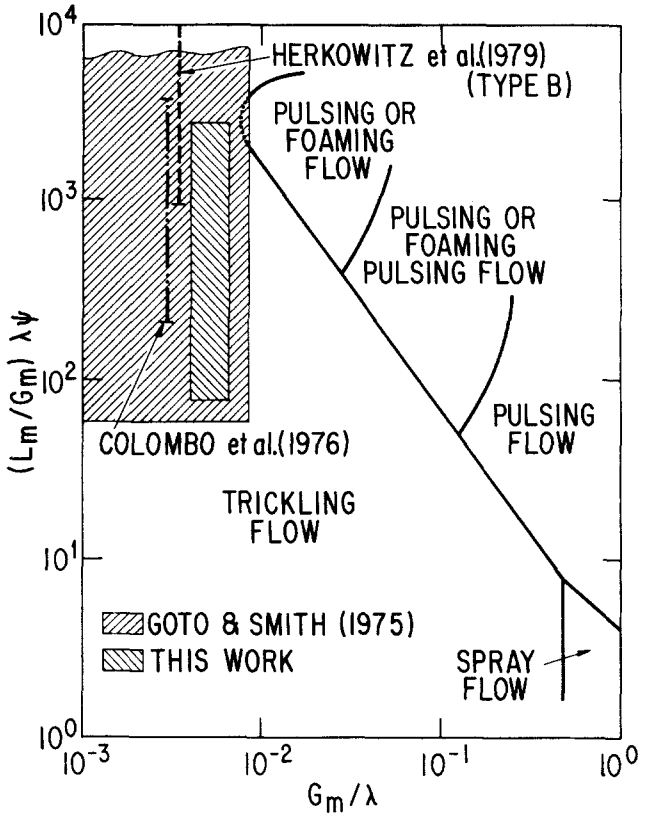

Figure 9. Flow regime of two-phase data according to the flow map of Charpentier et al. (1976).

$$H_T = H_S + A(u_L)^{1/3}(\mu_L)^{1/4} \tag{13}$$

The parameter A and total static holdup H_S were determined from the plots of H_T versus $(u_L)^{1/3}$ $(\mu_L)^{1/4}$ which yield straight lines. This allows the dynamic liquid holdup $H_D = H_T - H_S$ to be calculated.

The apparent data scatter was caused by a malfunctioning timing circuit and analog clock (data marked by triangles and diamonds). A much smoother trend was observed when a new quartz crystal-controlled clock was installed (data marked by squares and circles). The error bars for these former runs are larger than the data symbol which represents the mean value obtained at a given flow rate. However, the error bars are well within the data points for the latter runs.

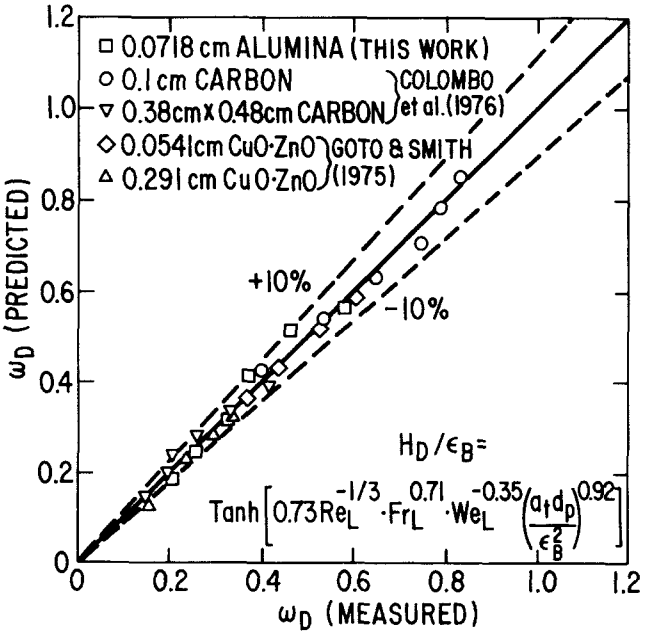

Figure 11. Comparison of predicted to measured values for dynamic saturation correlation.

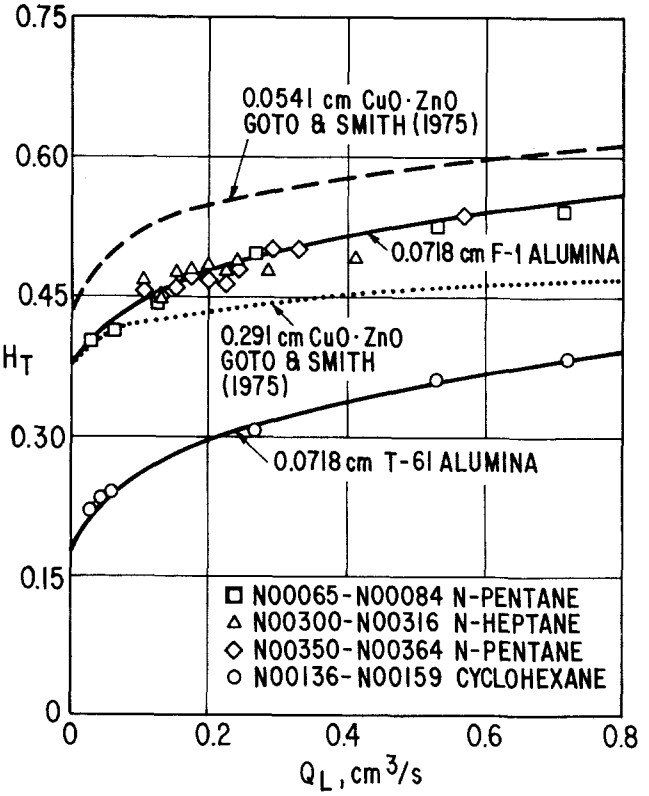

Figure 10. Total liquid holdup for various packings as a function of liquid volumetric flow rate.

TABLE 4. RANGE OF VARIABLES FOR DYNAMIC SATURATION CORRELATION

A. *Dimensionless Variables*		
	$0.3 \le \mathrm{Re}_L$	≤ 32
	$3.0 \times 10^{-5} \le \mathrm{Fr}_L$	$\le 2.2 \times 10^{-2}$
	$3.4 \times 10^{-7} \le \mathrm{We}_L$	$\le 9.1 \times 10^{-4}$
	$0.87 \le \frac{a_t d_p}{\epsilon_B^2}$	≤ 8.1
B. *Actual Variables*		
	$0.65 \le \rho_L$(g/cm^3)	≤ 1.0
	$0.32 \le \mu_L$(g/cm s)	≤ 0.96
	$0.054 \le d_p$(cm)	≤ 0.41
	$0.37 \le \epsilon_B$	≤ 0.52
	$0.08 \le \epsilon_P$	≤ 0.56

The equation of Satterfield and Way (1972) agrees with the holdup trends established by the data of Goto and Smith (1975) and of this study. However, this equation does not contain the basic dimensionless groups necessary for prediction of liquid holdup for other systems and involves an undetermined parameter A. Specchia and Baldi (1977) have recently proposed a correlation for dynamic saturation $\omega_D = H_D/\epsilon_B$ as a power function of the Galileo number Ga_L, Reynolds number Re_L, and packing characterization factor $a_t d_p/\epsilon_B$. This correlation yields an average relative error of -15.6% with a standard deviation of the error of 53.8% when applied to the data of Table 3. It was felt that a more suitable correlation could be obtained if a different form was used so that the dynamic saturation asymptotically approached unity at high liquid velocity. The following two forms were found to yield a more satisfactory correlation for the reported literature data on small porous particles (excluding the large absorption packing of Specchia and Baldi, 1977):

$$\omega_D = 1.0 - \exp\left[-0.634\ \mathrm{Re}_L^{-0.333}\mathrm{Fr}_L^{0.842}\mathrm{We}_L^{-0.448}\left(\frac{a_t d_p}{\epsilon_B^2}\right)^{1.086}\right] \quad (14)$$

$$\omega_D = \tanh\left[0.731\ \mathrm{Re}_L^{-0.333}\mathrm{Fr}_L^{0.708}\mathrm{We}_L^{-0.346}\left(\frac{a_t d_p}{\epsilon_B^2}\right)^{0.924}\right] \quad (15)$$

Equation 14 yielded an average error of 0.74% with an error standard deviation of 6.8% while Eq. 15 yielded an average error of 0.39% with a standard deviation of 6.2%. The agreement between the second correlation and data is presented in Figure 11. The range of dimensionless groups and actual physical properties over which the correlation was established are given in Table 4.

It should be noted that the packing characterization factor in this case was defined to be $a_t d_p/\epsilon_B^2$. This particular form yielded a relative error standard deviation which was approximately one-third of that obtained when the usual definition $a_t d_p/\epsilon_B$ was employed as the dimensionless group. This particular form, however, should not be regarded as final due to the limited data base upon which it was established.

b. Liquid-Solid Contacting. The estimates of liquid-solid contacting by the method of Schwartz et al. (1976) were obtained by applying Eq. 2 to the first moments for the adsorbing cyclohexene tracer and nonadsorbing pentane tracer at corresponding flow rates. The data are summarized in Table 5 and represented in Figure 12. It is apparent that liquid-solid con-

TABLE 5. SOLID-LIQUID CONTACTING EFFICIENCY VALUES OBTAINED FROM FIRST ABSOLUTE MOMENTS

Q_L (cm³/min)	$(\mu_1)_{ads}$ (s)	$(\mu_1)_{na}$ (s)	$(K_A)_{app.}$ (cm³/g)	$\eta_C = \dfrac{(K_A)_{app}^*}{(K_A)_{LF}}$
1.9184	1480.4	785.0	0.437	1.025
3.810	778.1	439.8	0.422	0.990
7.686	393.4	229.9	0.412	0.966
16.000	201.4	120.9	0.422	0.990
31.597	104.6	63.9	0.422	0.989
42.891	80.8	48.5	0.454	1.064
			Average: 0.428 ± 0.015	1.004 ± 0.035

* Based on $(K_A)_{LF}$ of 0.427 (cm³/g) obtained from liquid-filled column operation.

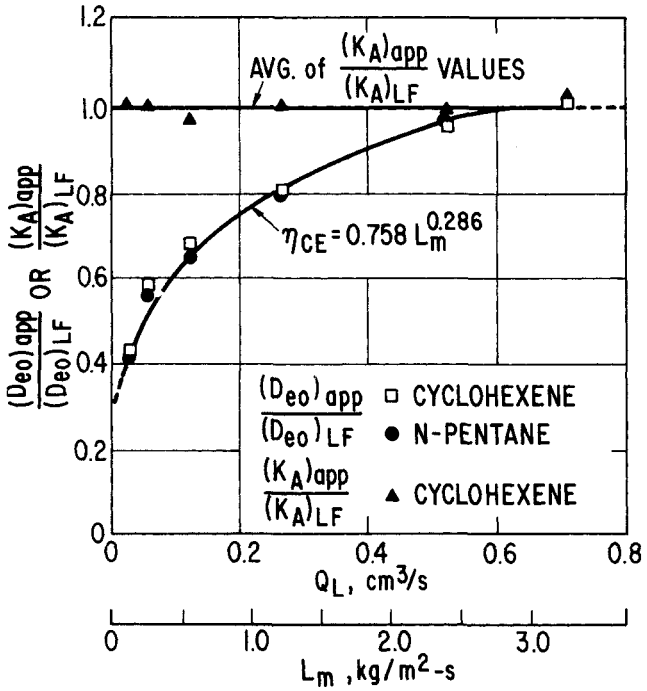

Figure 12. Comparison of $(D_{eo})_{app}/(D_{eo})_{LF}$ and $(K_A)_{app}/(K_A)_{LF}$ values for cyclohexene and n-pentane tracers.

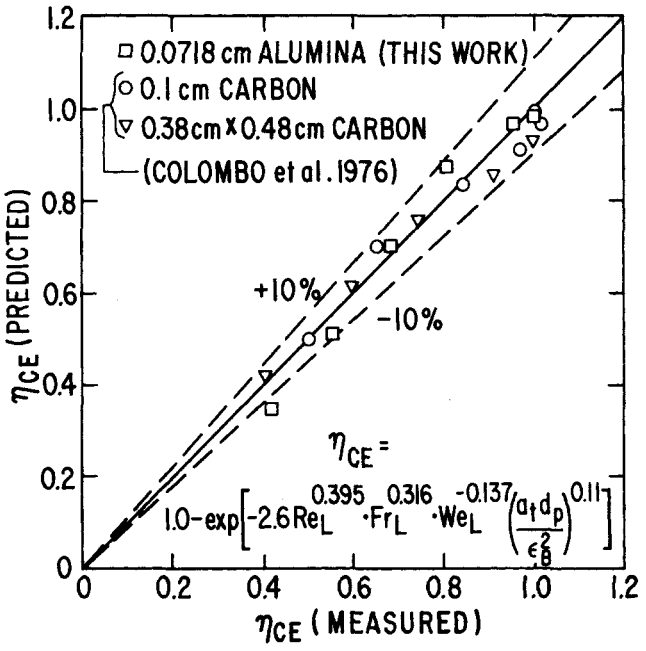

Figure 14. Comparison of predicted to measured values for solid-liquid contacting correlation ($\eta_{CE} = (D_{eo})_{app}/(D_{eo})_{LF}$).

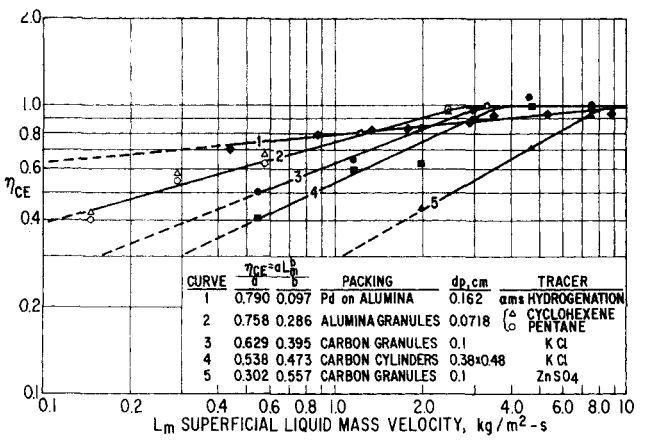

Figure 13. External solid-liquid contacting efficiency for various literature data as a function of superficial liquid mass velocity L_m ($\eta_{CE} = (D_{eo})_{app}/(D_{eo})_{LF}$).

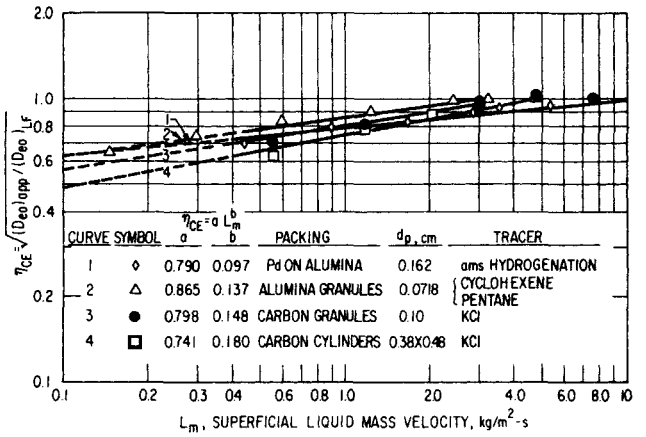

Figure 15. External liquid-solid contacting efficiency for various literature data as a function of superficial liquid mass velocity L_m ($\eta_{CE} = \sqrt{(D_{eo})_{app}/(D_{eo})_{LF}}$ and $\eta_{CE} = k_{app}/k_c$).

tacting defined by $(K_A)_{app}/(K_A)_{LF}$ does not exhibit any trend with flow rate and yields an average value of 1.004 ± 0.035 over the flow rate range examined. This indicates the absence of reactor-scale incomplete contacting, i.e., an internal contacting efficiency of unity. This also indicates that the catalyst internal pore structure is interconnected. The method cannot assess whether external contacting is complete since external area is negligible in comparison to internal area as indicated earlier.

Schwartz et al. (1976) reported a constant value of 0.65 for liquid-solid contacting over a similar range of liquid flow rates. A value less than unity may have been caused by either reactor-scale incomplete contacting or by a lower activation state of the alumina bed on which the two-phase runs were performed. As a consequence of this latter condition, $(K_A)_{app}$ determined from the alumina pellets in two-phase flow would be less than $(K_A)_{LF}$ obtained in batch adsorption-isotherm measurements.

That the ratio $(K_A)_{app}/(K_A)_{LF}$ is unity can also be shown for the data of Colombo et al. (1976) which was not done in their original paper. This confirms that their pellets were indeed completely internally wetted. In addition, the analysis of Colombo et al. (1976) can be applied to the variance of the impulse response curves obtained in this work. Application of Eq. 3 with the previously mentioned correlations for Pe_L and k_{LS} [neither of which had a significant effect on $(D_{eo})_{app}$] allowed the values of $(D_{eo})_{app}$ to be determined for pentane (nonadsorbing) and cyclohexene (adsorbing) tracer. The ratio of $(D_{eo})_{app}/(D_{eo})_{LF}$ is a strong function of liquid flow rate as illustrated in Figure 12 and, since the internal wetting was shown to be complete, must be a measure of external contacting efficiency.

Roberts and Yadwadkar (1972) showed that laminar film flow theory of a liquid rivulet over a plate could be used to relate external contacting to liquid superficial mass velocity by a simple power law equation of the form:

$$\eta_{CE} = a\, L_m^{\frac{3s-1}{2}} \tag{16}$$

The available holdup correlations suggested a value of s in the range from 0.5 to 0.75.

It was first assumed that the ratio of $(D_{eo})_{app}/(D_{eo})_{LF}$ is a direct measure of external contacting efficiency as suggested by Colombo et al. (1976). The next three figures are based on that assumption. Figure 12 demonstrates the Eq. 16 yields a satisfactory correlation for the external contacting when defined in the above manner. Figure 13 shows that all available literature data on external contacting are adequately represented by such a form. The tracer based curves 2-5 [$\eta_{CE} = (D_{eo})_{app}/(D_{eo})_{LF}$] seem to follow a trend. Curve 1, which was obtained by evaluating external contacting from reaction studies ($\eta_{CE} = k_{app}/k_v$), has a slightly different trend. If one disregards this later curve and curve 5, which even the authors could not explain, then for a given L_m the external contacting increases with decreasing particle size. This is consistent with the observation of Goto and Smith (1975) for liquid holdup and with the industrial practice of adding fines to improve contacting.

Several correlations (Shulman et al., 1955; Onda et al., 1967; Puranik and Vogelpohl, 1974) for external contacting of large non-porous packing ($d_p > 1.0$ cm) typical of absorption columns exist in the literature. None of these, however, includes data on small porous packing typical for trickle-bed reactors. The form of the correlation proposed by Onda et al. (1967) includes all of the pertinent dimensionless groups such as Re_L, Fr_L, We_L and σ_c/σ_L. The last ratio represents the ratio of critical to noncritical capillary number, Ca_c/Ca. This correlation form is equivalent to Eq. 14 presented in this paper for dynamic saturation so that it exhibits the proper asymptotic behavior. The information on critical surface tension for the data presented in Table 3 is lacking and such a correlation could not be attempted. Furthermore, it appears that external contacting should be a function of Reynolds, Froude, and Weber numbers and dynamic contact angle which is probably a function of Capillary number and packing characterization factor. Since the Capillary number is a ratio of Weber and Reynolds numbers, correlations of the type presented by Eqs. 14 and 15 were attempted. The following results were obtained using all the tracer based data of Table 3:

$$\eta_{CE} = \frac{(D_{eo})_{app}}{(D_{eo})_{LF}} = 1.0 - \exp\left[-2.6\ \mathrm{Re}_L^{0.395}\mathrm{Fr}_L^{0.316}\mathrm{We}_L^{-0.137}\left(\frac{a_t d_p}{\epsilon_B^2}\right)^{-0.11}\right] \tag{17}$$

$$\eta_{CE} = \frac{(D_{eo})_{app}}{(D_{eo})_{LF}} = \tanh\left[3.03\ \mathrm{Re}_L^{0.375}\mathrm{Fr}_L^{0.312}\mathrm{We}_L^{-0.122}\left(\frac{a_t d_p}{\epsilon_B^2}\right)^{-0.11}\right] \tag{18}$$

The agreement between the correlation given by Eq. 17 and data on which it is based is given in Figure 14. The relative error and standard deviation of the error is $0.83 \pm 6.5\%$ for each equation, respectively.

It should be noted that both Eqs. 17 and 18 are based on tracer data for the range of variables indicated in Table 4 which pertain to the non-interacting regime. In addition, both equations are based on the assumption that $(D_{eo})_{app}/(D_{eo})_{LF}$ is a direct measure of external contacting efficiency.

If one assumes the latest formulation by Baldi (1980), then contacting efficiency is given by $\sqrt{(D_{eo})_{app}/(D_{eo})_{LF}}$. This is plotted in Figure 15 and it seems that both tracer based data and reaction based data now indicate more similar trends. The reaction data of Herskowitz et al. (1979) were taken at a very high value of the modulus and are a good measure of external contacting efficiency. Since the square root of the diffusivity ratios brings both the reaction and tracer based contacting data into closer agreement, it seems that such a square root relationship is a better measure of external contacting efficiency. Correlations developed on this basis based on both reaction and tracer data are:

$$\eta_{CE} = \sqrt{(D_{eo})_{app}/(D_{eo})_{LF}} = 1.0 - \exp\left[-1.35\ \mathrm{Re}_L^{0.333}\mathrm{Fr}_L^{0.235}\mathrm{We}_L^{-0.170}\left(\frac{a_t d_p}{\epsilon_B^2}\right)^{-0.0425}\right] \tag{19}$$

$$\eta_{CE} = \sqrt{(D_{eo})_{app}/(D_{eo})_{LF}} = \tanh\left[0.664\ \mathrm{Re}_L^{0.333}\mathrm{Fr}_L^{0.195}\mathrm{We}_L^{-0.171}\left(\frac{a_t d_p}{\epsilon_B^2}\right)^{-0.0615}\right] \tag{20}$$

Both Eqs. 19 and 20 yielded an average error of 0.3% with standard deviation of 3.5%. One should recall, however, that five unknown constants were determined from 26 experimental points representing mean values from a total of about eighty experiments. Nevertheless, this correlation fits all small catalyst packing and reconciles reaction and tracer determined contacting efficiencies. The exact relationship between $(D_{eo})_{app}/(D_{eo})_{LF}$ and external contacting can only be obtained when the difficult transient diffusion problem for partially wetted catalysts is solved.

ACKNOWLEDGMENT

This work was partially supported by the National Science Foundation Grant ENG73-08284-A02 and by industrial funds from Amoco, Monsanto and Shell Development Company.

NOTATION

a_t = packing external surface area per unit volume of reactor, $S_{ex}(1 - \epsilon_B)/V_P$, m^{-1}

A = parameter in Eq. 13, $(cm/s)^{-1/3}\ (g/cm/s)^{-1/4}$

A_R = reactor inner cross-sectional area, m^2
C_L = tracer concentrations in the liquid at the reactor exit, mol m^{-3}
C_1 = constant in Eq. 8, dimensionless
Ca = Capillary number, ratio of viscous to surface tension forces, $We_L\ Re_L^{-1}$, dimensionless
d_p = catalyst particle diameter, m
D_{eo} = effective diffusivity of tracer in the pores of catalyst pellet based on total pellet cross-sectional area, $D_{eo} = D_m\epsilon_P/\tau$, m^2s^{-1}
D_m = molecular diffusivity of the tracer, m^2s^{-1}
D_{LO} = axial dispersion coefficient of the flowing liquid based on total reactor cross-sectional area, m^2s^{-1}
F_i = fraction of catalyst pore volume filled with liquid, dimensionless
Fr_L = Froude number for the liquid phase, $a_tL_m^2/\rho_L^2g$, dimensionless
G_m = superficial gas mass velocity, kg m^{-2} s^{-1}
H_D = dynamic liquid external holdup, (m^3 of flowing liquid)/(m^3 of bed volume), dimensionless
H_L = external liquid holdup, (m^3 of liquid external to the catalyst pellets)/(m^3 of bed volume), dimensionless
H_S = total static liquid holdup, (m^3 of stagnant liquid in and outside of the pellets)/(m^3 of bed volume), dimensionless
H_T = total liquid holdup, (m^3 of total liquid)/(m^3 of bed volume), dimensionless
k = first order reaction rate constant, (m^3 fluid)/(m^3 catalyst-second), s^{-1}
k_{LS} = liquid-to-solid mass transfer
k_v = first order reaction rate constant determined in liquid-full beds, s^{-1}
K_A = adsorption equilibrium constant, m^3 kg^{-1}
L = length of reactor packed section, m
L_m = superficial liquid mass velocity, kg m^{-2} s^{-1}
Pe_L = Peclet number for the liquid based on reactor length, u_LL/D_{LO}, dimensionless
Q_L = liquid volumetric flow rate, m^3s^{-1}
R = catalyst pellet radius, m
Re_L = Reynolds number based on particle diameter, $d_pu_L\rho_L/\mu_L$, dimensionless
S_{ex} = external surface area of the catalyst pellet, m^2
Sc_L = Schmidt number for the liquid, μ_L/ρ_LD_m, dimensionless
t = time, s
u_L = liquid superficial velocity, m s^{-1}
V = volume, m^3
V_p = pellet volume, m^3
V_R = unpacked reactor volume, m^3
We_L = Weber number for the liquid, $L_m^2/\sigma_L\rho_La_t$, dimensionless

Greek Letters

δ_1, δ_e, δ_i = parameters defined by Eqs. 4 through 6, s
δ_o = parameter defined by Eq. 7, dimensionless
ϵ_B = bed void fraction, (m^3 of voids external to the catalyst pellets)/(m^3 of bed volume), dimensionless
ϵ_P = porosity of catalyst particles, dimensionless
η_C = liquid-solid contacting efficiency based on total catalyst area, dimensionless
η_i = liquid-solid contacting efficiency based on internal catalyst area, dimensionless
η_{CE} = liquid-solid contacting efficiency based on external catalyst area, dimensionless
μ_L = liquid viscosity, kg m^{-1} s^{-1}
μ_n = n-th normalized absolute moment of the tracer impulse response curve defined by Eq. 9, s^n
ρ_L = liquid density, kg m^{-3}
σ_θ^2 = dimensionless variance, σ^2/μ_1^2, dimensionless
σ_L = surface tension for the liquid, kg m^{-1} s^{-1}
τ = mean residence time of tracer, $\tau = \mu_1$, s

Subscripts

app = apparent, evaluated in two-phase flow
C = refers to the packed bed (column) alone
D = refers to the system consisting of the packed bed and sampling and injection lines
D.V. = refers to the sampling and injection system alone
eo = based on total cross-sectional area of catalyst
L = refers to the liquid
LF = refers to liquid-full operation
SS = refers to sampling system
sys = refers to the total system consisting of packed bed plus all the sampling and injection lines

LITERATURE CITED

Baldi, G., "Design and Scale-up of Trickle-Bed Reactors. Solid-Liquid Contacting Effectiveness," Paper presented at the NATO Advanced Study Institute on Multiphase Chemical Reactors," Vimeiro, Portugal (Aug. 18-30, 1980).

Buffham, B. A., and M. N. Rathor, "The Influence of Viscosity on Axial Mixing in Trickle Flow in Packed Beds," *Transactions of the Institution of Chemical Engineers*, **56**, 266 (1978).

Chung, S. F., and C. Y. Wen, "Longitudinal Dispersion of Liquid Flowing Through Fixed and Fluidized Beds," *AIChE J.*, **14**, 857 (1968).

Colombo, A. J., G. Baldi, and S. Sicardi, "Solid-Liquid Contacting Effectiveness in Trickle-Bed Reactors," *Chem. Eng. Sci.*, **31**, 1101 (1976).

Duduković, M. P., "Catalyst Effectiveness Factor and Contacting Efficiency in Trickle-Bed Reactors," *AIChE J.*, **23 (6)**, 940 (1977).

Dwivedi, P. N., and S. N. Upadhyay, "Particle-Fluid Mass Transfer in Fixed and Fluidized Beds," *I&EC Process Design and Development*, **16 (2)**, 157 (1977).

Germain, A., G. L'Homme, and A. LeFebvre, "The Trickle-flow and Bubble-flow Reactors in Chemical Processing," *Chemical Engineering of Gas-Liquid-Solid Catalyst Reactions*, A. L'Homme, ed., p. 265, CEBEDOC, Liège (1979).

Gianetto, A., G. Baldi, V. Specchia, and S. Sicardi, "Hydrodynamics and Solid-Liquid Contacting Effectiveness in Trickle-Bed Reactors," *AIChE J.*, **24 (6)**, 1087 (1978).

Goto, S., and J. M. Smith, "Trickle-Bed Reactor Performance, Part 1. Holdup and Mass Transfer Effects," *AIChE J.*, **21 (4)**, 706 (1975).

Goto, S., J. Levec, and J. M. Smith, "Trickle-Bed Oxidation Reactors," *Cat. Rev.—Sci. Eng.*, **15**, 187 (1977).

Herskowitz, M., R. G. Carbonell, and J. M. Smith, "Mass Transfer and Partial Wetting in Trickle-Bed Reactors," *AIChE J.*, **25 (2)**, 272 (1979).

Hochman, J. M., and E. Effron, "Two-Phase Concurrent Downflow in Packed Beds," *I&EC Fundamentals*, **8**, 63 (1969).

Hofmann, H., "Hydrodynamics, Transport Phenomena, and Mathematical Models in Trickle-Bed Reactors," *Int. Chem. Eng.*, **17**, 19 (1977).

Hofmann, H., "Multiphase Catalytic Packed Bed Reactors," *Cat. Rev.—Sci. Eng.*, **17**, 71 (1978).

Koros, R. M., "Catalyst Utilization in Mixed Phase Fixed Bed Reactors," 4th Int. Symp. Chem. React. Eng., **I**, pIX-372, Dechema, Frankfurt (1976).

Krauze, R., and M. Serwinski, "Moistened Surface and Fractional Wetted Area of Ceramic Raschig Rings," *Inzynieria Chemiczna*, **1**, 415 (1971).

Lapidus, L., "Flow Distribution and Diffusion in Fixed-Bed Two-Phase Reactors," *Industrial and Engineering Chemistry*, **49**, 1000 (1957).

Mills, P. L., "Catalyst Effectiveness and Solid-Liquid Contacting in Trickle-Bed Reactors," D. Sc. thesis, Washington University, St. Louis, MO (May, 1980).

Mills, P. L., and M. P. Duduković, "A Modified Differential Refractometer For Continuous Liquid-Phase Residence Time Distribution Studies," *I&EC Fundamentals*, **18**, 292 (1979).

Mills, P. L., and M. P. Duduković, "Analysis of Catalyst Effectiveness in Trickle-Bed Reactors Processing Volatile or Nonvolatile Reactants," *Chem. Eng. Sci.* (1980).

Onda, K., H. Takeuchi, and Y. Kayama, "Effect of Packing Materials on the Wetted Surface Area," Kagaku Kogaku, **31**, 126 (1967).

Puranik, S. S., and A. Vogelpohl, "Effective Interfacial Area in Irrigated Packed Columns," *Chem. Eng. Sci.*, **29**, 501 (1974).

Reid, Robert C., J. M. Prausnitz, and T. K. Sherwood, *The Properties of Gas and Liquids*, 3rd ed., McGraw-Hill, New York, NY (1977).

Roberts, G. W., and S. R. Yadwadkar, "The Efficiency of Liquid-Solid Contacting in Trickle-Bed Reactors," National AIChE Meeting, Dallas, TX (Feb., 1972).
Satterfield, C. N., "Trickle-Bed Reactors," *AIChE J.*, **21**, 209 (1975).
Satterfield, C. N., and P. F. Way, "The Role of the Liquid Phase on the Performance of a Trickle-Bed Reactor," *AIChE J.*, **18**, 305 (1972).
Shah, Y. T., *Gas-Liquid-Solid Reactor Design*, McGraw-Hill, New York (1979).
Schiesser, W. E., and L. Lapidus, "Further Studies of Fluid Flow and Mass Transfer in Trickle Beds," *AIChE J.*, **7**, 163 (1961).
Schneider, P., and J. M. Smith, "Adsorption Rate Constants from Chromatography," *AIChE J.*, **14(5)**, 762 (1968).
Schwartz, J. G., E. Weger, and M. P. Dudukovič, "A New Tracer Method for the Determination of Liquid-Solid Contacting Efficiency in Trickle-Bed Reactors," *AIChE J.*, **22(5)**, 953 (1976).
Shulman, H. L., C. F. Ullrich, A. Z. Proulx, and J. O. Zimmerman, "Performance of Packed Columns. II. Wetted and Effective Interfacial Areas, Gas and Liquid Mass Transfer Rates," *AIChE J.*, **1**, 253 (1955).
Specchia, V., and G. Baldi, "Pressure Drop and Liquid Holdup for Two Phase Concurrent Flow in Packed Beds," *Chem. Eng. Sci.*, **32**, 515 (1977).
Specchia, V., G. Baldi, and A. Gianetto, "Solid-Liquid Mass Transfer in Concurrent Two-Phase Flow Through Packed Beds," *I&EC Process Design and Development*, **17 (3)**, 372 (1978).
Suzuki, M., and J. M. Smith, "Kinetic Studies by Chromatography," *Chem. Eng. Sci.*, **26**, 221 (1971).

Manuscript received July 3, 1980; revision received November 17 and accepted December 10, 1980.

Multistage Membrane Separation Processes for the Continuous Fractionation of Solutes Having Similar Permeabilities

ISAO NODA
and
CARL C. GRYTE
Department of Chemical Engineering and Applied Chemistry
Columbia University
New York, NY 10027

A new cascade configuration for the continuous membrane fractionation of solutes having similar permeabilities is proposed. In this scheme, solute selectivity is amplified by combining a concentrator and several mass exchangers (e.g., a reverse osmosis unit and hollow fiber dialyzers) to achieve a desired degree of separation. Separation efficiency of the new cascade is compared with that of a conventional counter-current cascade.

SCOPE

Liquid-phase membrane separation processes (such as dialysis, reverse osmosis, and ultrafiltration) utilize the difference in the membrane permeability of molecules as a basis for separation. In dialysis, the flux of solutes across a membrane is mainly controlled by diffusional transport. Large surface area membrane modules such as hollow fiber units (Mahon and Lipps, 1971; Breslau et al., 1975; Stevenson et al., 1975; and Viswanadhan and Kramer, 1975) are often used to compensate for the slow diffusion-controlled flux. Hollow fiber dialysis has been successfully used, for example, in artificial kidney hemodialysis (Babb et al., 1971) to remove membrane-permeable waste materials from the blood. The application of dialysis so far has been limited to the separation of highly permeable solutes from practically impermeable colloids and particulates because of the low solute selectivity of currently available membranes. It is very difficult to obtain an appreciable degree of separation of solutes by dialysis if the permeabilities of the solutes are relatively close.

A single separation unit often achieves only a limited degree of separation. In order to obtain a desired degree of separation, the units are usually cascaded to construct a multistaged unit which multiplies the separation effect of each stage. This technique to enhance the separation is used for many separation processes. Gas phase multistaged separations which exploit the kinetic properties of gases as a basis for separation, e.g., mass diffusion (Maier, 1939), thermal diffusion (Clausius and Dickel, 1939), and gaseous diffusion (Hertz, 1922), have been known for many years. These operations are often used for the separation of isotopes. In aqueous systems, Ohya and Sourirajan (1969) and Kimura et al. (1969) proposed a multistaged reverse osmosis process for the separation of solutes from solution. Dialysis, on the other hand, has been almost exclusively used as a single-staged operation for the separation of highly permeable solutes from impermeable solutes. This investigation extends the possible application of dialysis to the fractionation of solutes having similar permeabilities.

CONCLUSIONS AND SIGNIFICANCE

Continuous dialysis separation of solutes having similar membrane permeabilities can be achieved by a multistaged cascade operation of dialyzers coupled with several concentrators. The degree of solute separation is not increased by a multistaged continuous dialysis without a concentrator. Large numbers of concentrators are often required to achieve the desired degree of the separation of solutes if a conventional counter-current cascade configuration of concentrator-dialyzer pairs is used. In this report, a novel cascade configuration which requires fewer concentrators to obtain the same degree of separation is presented. The successful development of a scheme to reduce the requirement of the number of concentrators is rather important since the concentrators usually contribute greatly to the cost of the solute separation. The results of the analysis of the multistaged dialysis systems are given in the form of a McCabe-Thiele diagram. The feasibility of separating solutes having relatively similar permeabilities is shown.

0001-1541-81-4961-0904-$2.00.